Design of Integrated Fluorescent Estrogens: The Second Donor Effect on Absorption, Fluorescence, and Ground-State Molecular Orbital Properties of *trans*-4,4'-Methoxynitrostilbene Systems†

Gregory M. Anstead and John A. Katzenellenbogen*

Roger Adams Laboratory, Department of Chemistry, University of Illinois, Urbana, Illinois 61801
(Received: May 15, 1989)

In the design of inherently fluorescent ligands for the estrogen receptor, biological constraints limit to hydroxyl the functional groups that can be utilized as electron donors. In an attempt to optimize the fluorescent properties of such probes, we have studied the effect that a second alkoxy donor has on the fluorescence properties of two systems, peripherally located in a nitro-substituted diarylindene, and centrally located in a nitrostilbene. The second donor causes bathochromic shift in the absorbance spectrum (stilbene greater than diarylindene); however, the Stokes shift and fluorescence solvatochromism are less in the dual donor systems compared to the corresponding monodonor system. The fluorescence solvatochromism is investigated by using a model for solvent dispersive and dipole interactions. The relevant parameters are evaluated as follows: molecular geometry is obtained from X-ray crystallography, molecular mechanics, or semiempirical MO methods; molecular volumes are determined by molecular graphics; ground-state dipole moments calculated by the AM1 method; the noncollinearity of the ground- and excited-state dipoles is considered. This analysis rationalizes the effect of the second donor on reducing the fluorescence solvatochromism and demonstrates that the magnitude of this reduction depends on the conjugative contact of the second donor, being greater in the stilbene system than the diarylindene. Such an approach may be useful in the design of other fluorescent spectroscopic probes.

Introduction

There has been great interest in the development of an estrogen receptor (ER)-targeted fluorophore to determine the distribution of the ER in individual mammary tumor cells.[1] Such an assay would provide the clinician with prognostic information of value in the selection of the most effective treatment modality. Many of the fluorescent ligands that have been prepared consist of an estrogen linked to a fluorophore of proven biological utility (fluorescein, nitrobenzoxadiazole) by a spacer arm[1] (Figure 1). However, most of these compounds suffer from poor ER binding affinity (due to the huge structural perturbation of the native ligand), high nonspecific binding to nontarget proteins (as a consequence of the additional lipophilicity of the spacer arm and fluorophore), or quenching of the fluorescence upon ER binding (perhaps because the fluorophore is residing outside the binding pocket).[2]

An integrated fluorescent estrogen,[3] i.e., a compound in which the ligand and fluorophore are essentially congruent, may avoid these problems because molecular components in excess of the ligand itself are pared to a minimum and the fluorophore, by definition, will occupy the binding site. However, the design of such an integrated reagent is a tall order, requiring the simultaneous optimization of biological and fluorescence properties in a single structural manifold. In this paper the acquisition of desirable fluorescence characteristics (i.e., bathochromically shifted and environmentally sensitive emission[4]) in a prototypical integrated fluorescent estrogen is described.

The existence of long-wavelength emission and environmental sensitivity in a fluorophore requires the incorporation of distinct donor and acceptor moieties[5] at the termini of a conjugated system. In the development of donor/acceptor-substituted indenes (**1**) as integrated fluorescent estrogens,[6] we were confined by biological constraints to the use of the hydroxyl group, a weak donor (i.e., having high ionization potential).[7] To achieve high ER binding affinity, a ligand must possess a mimic of the phenol of estradiol (**2**);[8] analogues of estradiol with heteroatoms of greater donor strength (nitrogen[9] or sulfur[10]) at the crucial 3-position show weak ER-mediated biological activity.

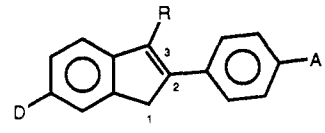

1, D = donor
A = acceptor
R = alkyl, aryl

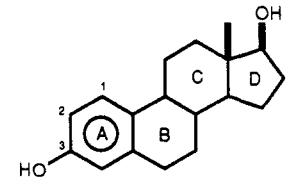

2

The absolute biological necessity of the hydroxyl group and its attendant poor donor properties will thereby limit the emission bathochromicity and environmental sensitivity that can be achieved in an integrated fluorescent estrogen. In an effort to circumvent these limitations, we have examined systems in which the phenol required for binding is retained, but a second donor[11] is affixed at another position.

Biological considerations also restricted the possible locations of a second donor. In general, the ER is intolerant of additional substitution on the A-ring of estradiol (or the A-ring mimic of nonsteroidal systems).[8,12] To avoid the steric and/or electronic

* Address correspondence to John A. Katzenellenbogen, Box 37, Roger Adams Laboratory, 1209 W. California Street, University of Illinois, Urbana, IL 61801.

† This paper is dedicated to Roger Adams, on the occasion of the 100th anniversary of his birthday, January 1989.

(1) (a) Fevig, T. L.; Lloyd, J. E.; Zablocki, J. A.; Katzenellenbogen, J. A. *J. Med. Chem.* **1987**, *30*, 156. (b) Fevig, T. L.; Mao, M. K.; Katzenellenbogen, J. A. *Steroids* **1988**, *51*, 471.

(2) Carlson, K. E.; Coppey, M.; Magdelenat, H.; Katzenellenbogen, J. A. *J. Steroid Biochem.* **1987**, *32*, 345.

(3) Katzenellenbogen, J. A. *Cancer Treat. Rep.* **1978**, *62*, 1243.

(4) Waggoner, A. S. In *Applications of Fluorescence in the Biomedical Sciences*; Taylor, D. L., Waggoner, A. S., Murphy, R. F., Lanni, F., Birge, R. R., Eds.; A. R. Liss: New York, 1986; pp 3-28.

(5) Weber, G.; Farris, F. J. *Biochemistry* **1979**, *18*, 3075.

(6) (a) Anstead, G. M.; Katzenellenbogen, J. A. *J. Phys. Chem.* **1988**, *92*, 6249. (b) Anstead, G. M.; Katzenellenbogen, J. A. *J. Med. Chem.* **1988**, *32*, 1754.

(7) Griffiths, J. *Colour and Constitution of Organic Molecules*; Academic Press: London, 1976.

(8) Fanchenko, N. D.; Surchak, S. V.; Shchedring, R. N.; Pivnitsky, K. K.; Novikov, E. A.; Ishkov, V. L. *Acta Endocrinol. (Copenhagen)* **1979**, *90*, 167.

(9) Solmssen, U. V. *Chem. Rev.* **1945**, *37*, 481.

(10) Terenius, L. *J. Med. Chem.* **1970**, *13*, 1246.

(11) Ferg-Forgues, S.; Le Bris, M.-T.; Guetté, J.-P.; Valeur, B. *J. Phys. Chem.* **1988**, *92*, 6233.

(12) (a) Hahnel, R.; Twaddle, E.; Ratajczak, T. *J. Steroid Biochem.* **1973**, *4*, 21. (b) Heiman, D. F.; Senderoff, S. G.; Katzenellenbogen, J. A.; Neeley, R. J. *J. Med. Chem.* **1980**, *23*, 994.

0022-3654/90/2094-1328$02.50/0

SCHEME I

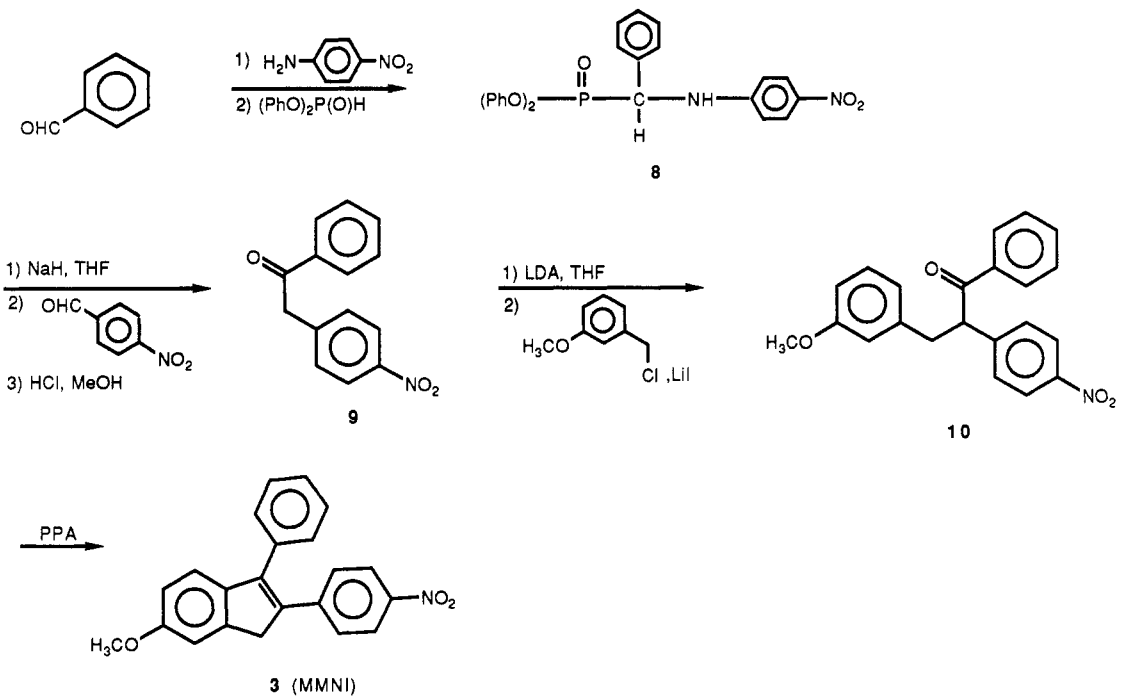

TABLE I: Absorbance Characteristics of the Lowest Energy $\pi \rightarrow \pi^*$ Band of the Methoxynitrostilbene Systems 3 and 5–7

	3 (MMNI)			5 (DMNI)[a]	6 (BIF)			7 (PNS)[a]
solvent	ν, 10^3 cm^{-1}	λ, nm	log ϵ^b	ν, 10^3 cm^{-1}	ν, 10^3 cm^{-1}	λ, nm	log ϵ^b	ν, 10^3 cm^{-1}
cyclohexane	25.51	392	4.35	25.25	25.64	390	4.35	27.93
CCl_4	25.25	396	4.33	25.00	25.38	394	4.29	27.78
benzene	25.00	400	4.29	24.75	24.88	402	4.28	27.32
ether	25.64	390	4.32	25.25	25.38	394	4.29	27.93
dioxane	25.25	396	4.32	25.00	25.13	398	4.26	27.47
THF	25.13	398	4.31	24.75	24.75	404	4.30	27.32
EtOAc	25.38	394	4.31	25.51	24.88	402	4.31	27.32
$CHCl_3$	24.75	404	4.26	24.51	24.63	406	4.26	27.17
CH_2Cl_2	24.88	402	4.29	24.51	24.50	408	4.29	27.03
acetone	25.13	398	4.26	24.88	24.75	404	4.28	27.47
CH_3CN	25.25	396	4.29	24.88	24.63	406	4.27	27.32
n-BuOH	25.13	398	4.26	24.75	24.88	402	4.29	27.47
EtOH	25.25	396	4.30	24.88	24.88	402	4.27	27.47

[a] Reference 6a. [b] Extinction coefficient.

disruption produced by A-ring substitution, we have utilized alternate positions in two stilbene-type systems that are models of integrated fluorescent estrogens. In this paper, the absorption, fluorescence, and electronic characteristics of such mono- and dual-donor stilbenoid systems are described.

Nitroindene **3** (MMNI = *mono*methoxy*n*itroindene) is the donor/acceptor variant of the moderate affinity ER ligand **4**.[13]

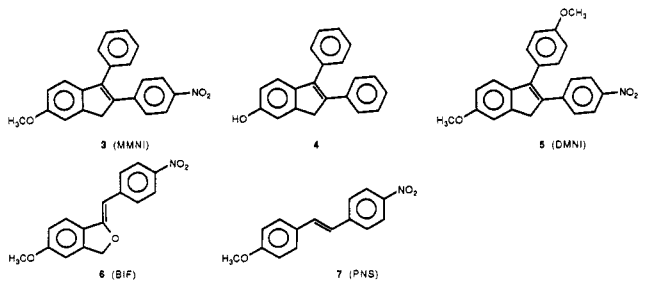

We have compared this monodonor compound to its dual donor analogue **5** (DMNI = *dim*ethoxy*n*itro*i*ndene).[6] Benzoisofuran (**6**) (BIF = *b*enzo*i*so*f*uran) with the second donor attached directly to the double bond, is compared to its stilbene analogue **7** (PNS = *p-n*itro*s*tilbenol).[6a] We have examined the methyl ethers of these systems instead of the more biologically relevant phenols because of their greater chemical stability; the ionization potentials (donor strengths) are similar.[7]

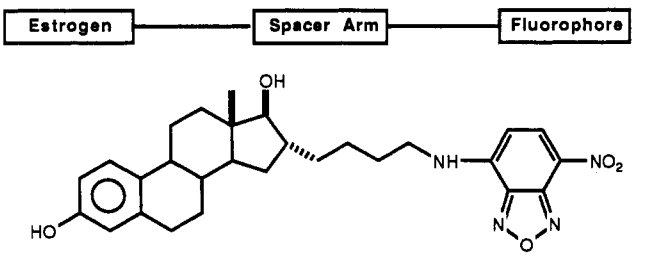

Figure 1. General form and a specific example of a conjugated fluorescent estrogen.[1]

Results and Discussion

Synthesis. *p*-Nitrostilbene (**7**) (PNS) and dimethoxynitroindene (**5**) (DMNI) were prepared as previously described.[6a] Monomethoxynitroindene (**3**) (MMNI) was synthesized as summarized in Scheme I. The requisite deoxybenzoin (**9**) was prepared by phosphonate carbanion methodology;[14] subsequent benzylation

(13) Anstead, G. M.; Altenbach, R. J.; Wilson, S. W.; Katzenellenbogen, J. A. *J. Med. Chem.* **1988**, *31*, 1316.

(14) Zimmer, H.; Nene, D. M. *Chimia* **1977**, *31*, 330.

SCHEME II

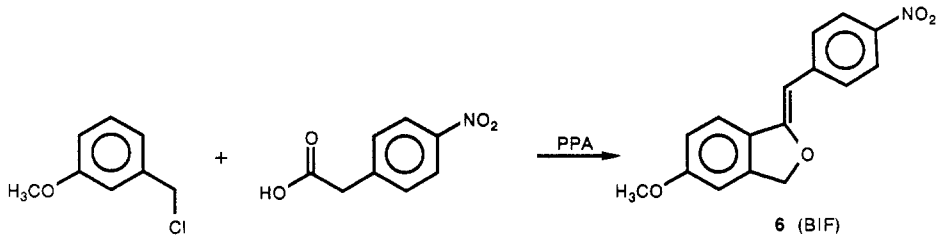

6 (BIF)

TABLE II: Infrared Stretching Frequencies of the Nitro Group in the Methoxynitrostilbene Systems and Related Compounds

	band position, cm^{-1}	
	asym	sym
PNS (7)	1511	1340
BIF (6)	1502	1335
MMNI (3)	1510	1341
DMNI (5)	1506	1337
nitrobenzene[a]	1520	1345
p-nitroaniline[a]	1475	1310

[a] Reference 16.

and cyclodehydration afforded the indene.

Benzoisofuran (6) (BIF) was prepared in one pot by reacting *p*-nitrophenylacetic acid with 3-methoxybenzyl chloride in polyphosphoric acid (PPA). Initially, acylation occurs para to the methoxy group. This is followed by enolization and O-alkylation (see Scheme II).

Absorption Spectra. The absorption spectra of BIF and MMNI were measured in a number of solvents of varying polarity. The maxima of the lowest energy $\pi \rightarrow \pi^*$ band are recorded in Table I. The maxima of PNS and DMNI are included for comparison purposes.

From a comparison of MMNI with DMNI, it can be seen that the second methoxy group attached to the para position of the 3-aryl ring in DMNI produces an additional bathochromic shift of ca. 370 cm^{-1}. However, the second donor in BIF, attached directly to the double bond, bathochromically shifts the maximum by about 2500 cm^{-1} over that of the monodonor stilbene PNS. For all four compounds, the position of the absorption maximum is not very sensitive to the solvent polarity.

According to Carsey et al.,[15] for donor/acceptor-substituted benzenes, the lower the energy of the longest wavelength $\pi \rightarrow \pi^*$ band, the more polar the ground state. Carsey also stated that this generalization was valid for a donor/acceptor (D/A) index, a term describing the extent of charge transfer. Thus, the order of ground-state polarity for these compounds is BIF = DMNI > MMNI > PNS. Since the acceptor, a *p*-nitrophenyl group, is the same in all cases, the donor strength and extent of charge transfer for the equilibrium ground state to Franck–Condon excited-state transition also follow this same order.

Infared Spectra. The asymmetric and symmetric N–O stretch bands of aromatic nitro groups are shifted to lower frequencies by electron donation.[16] Thus BIF, with a second donor, absorbs at lower frequencies than PNS (Table II). DMNI and MMNI have more similar frequencies, indicating the lesser donor effect for the *p*-methoxy group of the indene as compared to the enol ether oxygen of BIF. The stilbenes and indenes cannot be directly compared because the nitro stretch bands are also sensitive to conjugation;[16] the indene nitro groups may also be influenced by the conjugating 3-aryl substituent or torsional changes in the *trans*-stilbene system.

Emission Spectra. The emission spectra of MMNI and BIF were obtained in solvents of varying polarity. The emission maxima are listed in Table III, with those of DMNI and PNS included for comparison.

To understand the trends in the polarity sensitivity and bathochromicity of the emission in these compounds, it is best to analyze data only from those solvents that do not display special solvent effects (e.g., hydrogen bonding, special dispersive forces); this leaves the following group of well-behaved solvents: cyclohexane, ether, THF, ethyl acetate, acetone, and acetonitrile.[17] In these solvents, the emission maxima of DMNI are only slightly lower in energy (more bathochromic) than those of MMNI. Except in cyclohexane, the Stokes shift of MMNI exceeds that of DMNI. In the well-behaved solvents, the emission of BIF is not as bathochromic as that of PNS, and the Stokes shifts of BIF are much less. Thus, despite the larger increase in the bathochromicity of the absorption maximum for BIF, the second donor decreases the emission red shift.

The fluorescence solvatochromism (i.e., the change in the emission energy for a given change in solvent polarity) was assessed in the well-behaved solvents by a plot of ν_f vs π^*, an empirical solvent polarity–polarizability parameter.[17] The slope of such a plot is a measure of the relative fluorescence solvatochromism. The results appear in Table IV. The plots suggest that in both comparisons of monodonor and dual-donor systems, the dual-donor compound is less solvatochromic than its monodonor counterpart. Thus, the dual-donor systems, despite their increased absorption bathochromicity, have similar or less bathochromically shifted emission maxima and lesser Stokes shifts, and display less fluorescence solvatochromism than the corresponding monodonor systems. It was of interest to understand the molecular characteristics responsible for these effects.

Quantitative Aspects of Fluorescence Solvatochromism. The extreme solvent dependence of the emission of these dyes is indicative of intramolecular charge transfer in the excited state. The large excited-state dipole moment causes solvent reorientation. At equilibrium, this solvent relaxation is complete, and the more polar solvent will stabilize the excited state more effectively, producing a larger Stokes shift.[19]

There have been many quantitative treatments of solvent dispersive and dipole interactions on the excited state.[19,20] The molecules considered in this study do not present C_{2v} symmetry, and thus the ground- and excited-state dipole moments are not collinear.[21] Equation 1[20,22] addresses this situation; ν_a and ν_f refer

$$\nu_a - \nu_f = (2/hca^3)(\mu_g^2 + \mu_e^2 - \mu_g\mu_e \cos\alpha) \times \left[\frac{D-1}{D+2} - \frac{n^2-1}{n^2+2}\right]\frac{(2n^2+1)^2}{(n^2+2)^2} + \text{const} \quad (1)$$

to the absorption and emission frequencies, D and n are the solvent dielectric constant and refractive index, μ_g and μ_e are the ground- and excited-state dipole moments, a is the Onsager cavity radius, and α is the angle between μ_g and μ_e. The equation can be manipulated to solve for μ_e and α.[22]

(15) Carsey, T. P.; Findley, G. L.; McGlynn, S. P. *J. Am. Chem. Soc.* **1979**, *102*, 4502.
(16) Silverstein, R. M.; Bassler, G.; Morrill, T. C. *Spectrometric Identification of Organic Compounds*, 4th ed.; Wiley: New York, 1981.
(17) Abboud, J. L.; Kamlet, M. J.; Taft, R. W. *J. Am. Chem. Soc.* **1977**, *99*, 8325.
(18) (a) Balter, A.; Nowak, W.; Pawelkiewicz, W.; Kowalczyk, W. *Chem. Phys. Lett.* **1988**, *143*, 565. (b) Le Bris, M.-T.; Mugnier, J.; Bourson, J.; Valeur, B. *Chem. Phys. Lett.* **1984**, *106*, 124.
(19) Lakowicz, J. R. *Principles of Fluorescence Spectroscopy*; Plenum: New York, 1983.
(20) Bakhshiev, N. G.; Knyazhanskii, M. T.; Minkin, V. I.; Osipov, O. A.; Saidov, G. V. *Russ. Chem. Rev.* **1969**, *38*, 740.
(21) Liptay, W. *Excited States* **1974**, *1*, 128.
(22) Meech, S. R.; O'Connor, D. V.; Phillips, D. *J. Chem. Soc., Faraday Trans. 1* **1983**, *79*, 1563.

TABLE III: Emission Properties of Methoxynitrostilbene Systems

	3 (MMNI)				6 (BIF)			
solvent	ν, 10^3 cm^{-1}	λ, nm	Stokes shift,[b] cm^{-1}	5 (DMNI)[a] ν, 10^3 cm^{-1}	ν, 10^3 cm^{-1}	λ, nm	Stokes shift,[b] cm^{-1}	7 (PNS)[a] ν, 10^3 cm^{-1}
cyclohexane	21.01	476	4500	19.72	20.33	492	5310	20.12
CCl_4	18.94	528	6310	19.42	20.88	479	4500	20.24
benzene	19.31	518	5700	18.66	20.08	498	4800	20.24
ether	19.57	511	6070	19.23	20.28	493	5100	20.20
dioxane	18.94	528	6310	17.89	19.80	505	5330	19.88
THF	17.79	562	7340	17.54	19.19	521	5560	19.08
EtOAc	17.70	565	7680	17.57	19.23	520	5650	19.23
$CHCl_3$	16.00	625	8750	15.85	17.45	573	7180	17.27
CH_2Cl_2	15.95	627	8930	15.77	17.39	575	7110	16.95
acetone	16.24	616	8890	16.18	17.51	571	7240	16.84
CH_3CN	15.22	657	10030	15.15	16.34	612	8290	15.46
n-BuOH	16.13	620	9000	16.34	16.75	597	8130	16.00
EtOH	16.47	607	8780	16.00	16.53	605	8350	15.50

[a] Reference 6a. [b] Energy(absorbance) − energy(emission).

TABLE IV: Results of a Plot of ν_f vs π^*[a] for the Methoxynitrostilbene Systems[b]

	PNS (7)	BIF (6)	MMNI (3)	DMNI (5)
slope	−5337	−4606	−6823	−5469
r[c]	0.86[d]	0.89	0.99	0.96

[a] Empirical solvent polarity–polarizability parameter. [b] Well-behaved solvents only (see text). [c] Correlation coefficient. [d] If the data from cyclohexane (for which the band shape is considerably different) is omitted from the regression analysis, the slope is −8465 and r = 0.93. Anomalous emissive behavior of fluorophores in cyclohexane has also been reported by others (ref 18).

However, eq 1 is derived for a spherical molecular shape, a poor approximation for the molecules in the current study. Alternatively, eq 2[23,24] applies for ellipsoidal molecules

$$\nu_a - \nu_f = (2/hca^3(\mu_e - \mu_g)^2 f(D,n) + \text{const} \qquad (2)$$

where

$$f(D,n) = \frac{2n^2+1}{n^2+2}\left[\frac{D-1}{D+2} - \frac{n^2-1}{n^2+2}\right] \qquad (3)$$

and the other terms are defined as for eq 1 (except a is the long axis radius of an ellipsoid). A plot of $\nu_a - \nu_f$ versus $f(D,n)$ for a series of solvents yields a slope from which the value of $(\mu_e - \mu_g)^2$ can be determined. An ellipsoidal shape is a good approximation for PNS and BIF, but MMNI and DMNI deviate from this idealized geometry.[6a] Also, eq 2 neglects cos α. Nevertheless, α can be estimated[25] from the position of μ_g (obtained from MO calculations) and the assumption that the main charge transfer in the first excited singlet state proceeds from the aromatic nucleus to the acceptor.[26] In any case, for small values of α, cos α is a negligible factor.

Equations 1 and 2 produce the following consequencies: (1) as α and a^3 increase, fluorescence solvatochromism decreases; and (2) as the difference between μ_g and μ_e ($\Delta\mu$) increases, fluorescence solvatochromism increases.[27] Both equations simplistically treat molecules as point dipoles[28] and ignore the change in the polarizability of the solute in different solvents.[29] Herein, eq 2 will be used to calculate μ_e; α will be evaluated as described above.

MO Calculations. The molecular volume a^3 can be obtained by using molecular graphics techniques on a molecule in which the geometry has been determined by force field or quantum mechanical methods or by X-ray crystallography. PNS and BIF are small enough systems to allow total geometry optimization by semiempirical MO calculations. The structures of PNS and BIF were first energy minimized by the MAXIMIN minimizer using the Tripos force field[30] within the SYBYL (version 3.4) molecular graphics program and then subjected to total geometry optimization by the AM1 MO method.[31] The larger size of MMNI

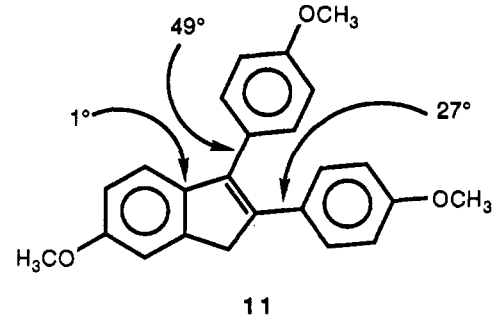

11

Figure 2. Normalized torsional angles of the aromatic rings with respect to the double bond in 2,3-bis(4-methoxyphenyl)-6-methoxyindene.[13]

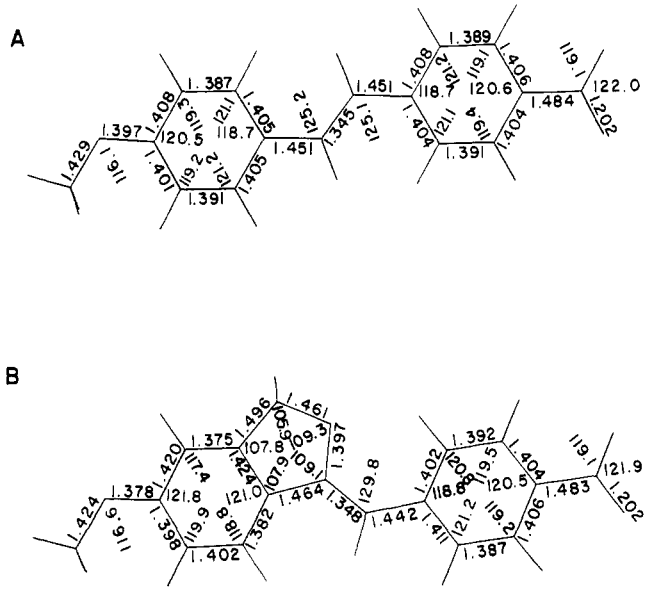

Figure 3. Optimized molecular geometries, bond lengths, and bond angles for PNS (7) (A) and BIF (6) (B) obtained from AM1 calculations. These geometries were used in the molecular volume determinations.

(23) Kawski, A. *Acta Phys. Polon.* **1966**, *29*, 507.
(24) Walker, M. S.; Miller, R. K.; Kudes, J. E. *J. Phys. Chem.* **1972**, *76*, 2240.
(25) Suppan, P. *Chem. Phys. Lett.* **1983**, *94*, 272.
(26) Exner, O. *Dipole Moments in Organic Chemistry*; Thieme: Stuttgart, 1975.
(27) Bakhshiev, N. G. *Opt. Spectrosc.* **1962**, *13*, 104. (b) Bakhshiev, N. G. *Opt. Spectrosc.* **1962**, *13*, 24.
(28) Rettig, W. *J. Mol. Struct.* **1982**, *84*, 303.
(29) Brady, J. E.; Carr, P. W. *J. Phys. Chem.* **1985**, *89*, 5759.
(30) Vinter, J. G.; Davis, A.; Saunders, M. R. *J. Comput.-Aided Mol. Des.* **1987**, *1*, 31.

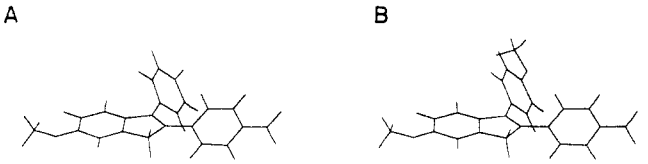

Figure 4. Molecular geometries of MMNI (**3**) (A) and DMNI (**5**) (B) used in the AM1 calculations and molecular volume determinations. This figure is also a stereoscopic representation of the 2,3-diarylindene geometry.

TABLE V: Molecular Volumes of the Methoxynitrostilbene Systems[a]

	PNS (7)	BIF (6)	MMNI (3)	DMNI (5)
vol, Å^3	217.9	230.8	292.7	307.9

[a] Calculated by the VOLUME command of the SYBYL molecular graphics package.

and DMNI rendered geometry optimization impractical in terms of computing time. For these systems, the molecular geometry was based on the X-ray crystallographic structure of the analogous trimethoxyindene (**11**)[13] (Figure 2), with appropriate group deletions and attachments. The structures of MMNI and DMNI thus obtained were subjected to a single self-consistent-field calculation by the AM1 method. The MO calculations provided the magnitude and direction of the ground-state dipole moment.

Molecular Structures. The structures of PNS and BIF obtained from the AM1 calculations appear in Figure 3. The molecules are essentially planar, like *trans*-stilbene.[32] The calculated Ar–O bond lengths are 1.397 and 1.378 Å for PNS and BIF, compared to an average of 1.371 Å for other methoxy aromatics.[33] The longer C=C bond lengths (1.345 and 1.348 Å for PNS and BIF) compared to *trans*-stilbene (1.341 Å)[32] and the shortening of the central bonds in the aromatic rings in both compounds suggest some quinoidal character in the ground state, as observed in other para-substituted aromatics.[34]

The geometries of MMNI and DMNI used in the AM1 calculations are shown in Figure 4. This geometry may not be ideal; nitro substitution is known to induce torsional changes in conjugated systems.[35] An inaccurate assessment of the pendant ring torsion will minimally affect the overall molecular volume,[6a] but may produce a large change in μ_g.[36]

Molecular Volumes. Molecular volumes were generated from the molecular structures by using Gaussian functions surface-contoured at a level representative of the van der Waals radii.[37] The results are summarized in Table V. In comparing the monodonor and dual-donor system, the dual-donor compound in each case is only slightly more voluminous. Thus, the size difference produces only a minor effect on the solvatochromism in the comparison of these monodonor and dual-donor systems. The principal determinant of the difference in solvatochromism of the monodonor and dual-donor systems must lie in the dipole moment terms μ_g, μ_e, and a. However, the molecular volume may contribute to the difference in solvatochromism between the diarylindene and stilbene fluors.

Ground-State Dipole Moments. The net ground-state dipole moment and the x, y, and z components of this moment were computed by the AM1 method (Table VI). The dipole moment obtained for PNS (7.06 D) agrees well with the value of 6.97 D, calculated by Ulman[38] using the AM1 method. Furthermore, the calculated values of μ_g for all four compounds are fairly consistent with the order of ground-state polarity assigned from the position of the absorption maximum (vide supra).

TABLE VI: Ground-State Dipole Moments, Components, and Angles

	μ_g,[a] D	C_x[b]	C_y[c]	C_z[d]	θ,[e] deg	μ_g(cor),[f] D
PNS (7)	7.06[g]	−4.86	5.10	0.361	133.5	5.78
BIF (6)	9.77	9.22	−3.22	0.258	19.3	7.95
MMNI (3)	7.24	−2.29	6.87	−0.327	108.4	5.92
DMNI (5)	8.59	−2.34	8.25	0.379	105.8	7.00

[a] Ground-state dipole moment from AM1 calculations. [b–d] x, y, and z components of μ_g, respectively. [e] Angular displacement of μ_g. [f] Corrected dipole moment based on eq 4. [g] An experimental dipole moment of 5.51 D was reported by Ulman.[38]

TABLE VII: Excited-State Dipole Moments for PNS, BIF, MMNI, and DMNI[a]

	m,[b] cm^{-1}	r[c]	$\Delta\mu$,[d] D	μ_e,[e] D	α,[f] deg
PNS (7)[g]	8580.1	0.96	13.6	19.4	14
BIF (6)	3294.9	0.81	8.69	16.6	3
MMNI (8)	6151.4	0.98	13.4	19.3	10
DMNI (6)	4752.8	0.94	12.1	19.1	15

[a] Calculated using eq 2 and 3, the solvent parameters from ref 40, the molecular volumes of Table V, the corrected ground-state dipole moments (Table VI), and the computational method of Lakowicz.[19] [b] Slope of plot for well-behaved solvents. [c] Correlation coefficient. [d] Defined as $\mu_e - \mu_g$. [e] Excited-state dipole moment. [f] Angle between μ_g and μ_e. [g] Data for cyclohexane omitted from the regression analysis (see footnotes of Table IV).

However, Ulman[38] found that, for an extensive series of para-substituted and para,para′-disubstituted stilbenes, the AM1 method consistently produced ground-state dipole moments greater than the experimentally determined moment. This data fits the regression equation

$$\mu_{exp} = 0.8\mu_{calcd} + 0.13 \qquad (r = 0.96) \qquad (4)$$

where μ_{exp} and μ_{calcd} are the experimental and calculated ground-state dipole moments and r is the correlation coefficient. If PNS, BIF, MMNI, and DMNI behave similarly, the ground-state dipole moments may be corrected by the use of eq 4 (Table VI).

In determining the direction of the ground-state dipole moments (Figure 5), the z component can be ignored in each case because it is small relative to the x and y components. This allows the ground-state dipole moment to be expressed simply in the xy plane instead of three-dimensionally. By use of the atom designated by the AM1 program as the 0,0,0-point of the Cartesian coordinate system, and the x and y components of the dipole moment, the direction of the dipole moment is provided by the vector relationship

$$C_x/\mu_g = \cos\theta$$

where μ_g is the ground-state dipole moment, C_x is the x component of μ_g, and θ is the angular displacement of μ_g from the x axis.

Excited-State Dipole Moments. Using eq 2 and 3 and the data from Tables I and III (well-behaved solvents only), we obtained the values of $\Delta\mu$ and μ_e for each of the four molecules (Table VII). The plots obtained by using eq 2 provide the correct trend of the variation of Stokes shift with $f(D,n)$, but the points tend to be scattered, common in many applications of a continuum model of solute–solvent interactions.[6a] The angle α between μ_g and μ_e was estimated from the intersection of μ_g (Figure 5A–D) with μ_e (assumed to be collinear with the Ar–NO_2 bond axis).

Bakhshiev[27b] calculated $\Delta\mu$ and μ_e for PNS as 12.5 and 18 D, respectively, with eq 1. We have previously determined $\Delta\mu$ and

(31) Dewar, M. J. S.; Zoebisch, E. G.; Healey, E. F.; Steward, J. J. P. *J. Am. Chem. Soc.* **1985**, *107*, 3902.
(32) Hoekstra, A.; Meertens, P.; Vos, A. *Acta Crystallogr.* **1975**, *B31*, 2813.
(33) Nyburg, S. C.; Faerman, C. H. *J. Mol. Struct.* **1986**, *140*, 347.
(34) Malar, E. J. P.; Jug, K. *J. Phys. Chem.* **1985**, *89*, 5235.
(35) Buchanan, G. W.; Montaudo, G.; Finocchiaro, P. *Can. J. Chem.* **1974**, *52*, 767.
(36) Eckert, C.; Heisel, F.; Miehé, J. A.; Lapouyade, R.; Ducasse, L. *Chem. Phys. Lett.* **1988**, *153*, 357.
(37) *SYBYL Molecular Modeling Software, Version 3.4*; Tripos Associates: St. Louis, MO, 1987.
(38) Ulman, A. *J. Phys. Chem.* **1988**, *92*, 2385.
(39) Dominey, L. A.; Comeford, L.; Chen, S. J-H.; Grunwald, E. *J. Phys. Chem.* **1987**, *91*, 2211.
(40) Krstulovic, A. M.; Brown, P. R. *Reversed-Phase High-Performance Liquid Chromatography*; Wiley: New York, 1982.

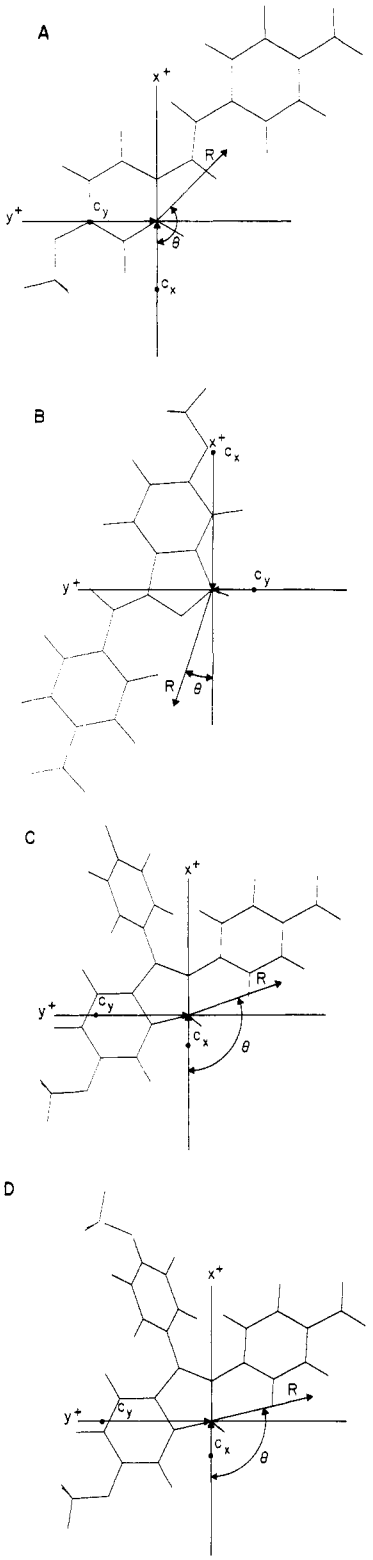

Figure 5. Direction of ground-state dipole moments in PNS (A), BIF (B), MMNI (C), and DMNI (D). The resultant R of the two component vectors C_x and C_y is equivalent to the ground-state dipole moment vector. Dipole vectors point from positive to negative pole, following physical–organic convention.[39]

μ for PNS and DMNI, using eq 2 and uncorrected MNDO[41] values for μ_g.[6a]

The greater fluorescence solvatochromism of PNS compared to BIF is explicable from the $\Delta\mu$ term. The fluorescence solvatochromism of MMNI is only slightly greater than that of DMNI, as the more similar values of $\Delta\mu$ attest. In assessing the factors responsible for the disparity in fluorescence solvatochromism between the monodonor and dual-donor systems, α and volume are not very significant for the examples presented herein; the magnitudes of μ_g and μ_e are the important terms. It is not valid to compare the stilbene and diarylindene fluors quantitatively, because of the shape differential among these classes of molecules.

Ionization Potentials. Absorption spectra and ionization potentials are regarded as sensitive indicators of orbital interactions in molecules.[42] The ionization potentials for PNS, BIF, MMNI, and DMNI, as determined in the AM1 calculations, are 8.76, 8.68, 8.59, and 8.74 eV, respectively. Thus, despite its effect on the absorption spectra, the second donor seems to have little effect on the overall ionization potential. The AM1 method is reported to successfully predict trends for ionization potential in conjugated molecules.[43]

Conclusions

In this study, several methods were integrated to facilitate the understanding of structural effects on fluorescence solvatochromism. First, only solvents which display no special dispersive forces were used in the correlations.[17] The molecular geometry was not estimated, but assigned using X-ray crystallography, molecular mechanics, or the most modern available semiempirical MO method (AM1).[31] The molecular volumes were determined directly by molecular graphics techniques. Ground-state dipole moments were calculated by the AM1 method and corrected empirically.[38] Finally, the noncollinearity of the ground-state and excited dipole moments was addressed.[25] Nevertheless, this analysis suffers from the inherent limitations of a continuum model of solvent effects, based on Onsager reaction field theory.[6a,28,29] Our methodology may be improved by taking spectral measurements in a more extensive set of well-behaved solvents, by using the center of gravity of the emission band instead of the maximum,[22] or by adopting features of the MSI model,[28] which considers actual molecular shape and charge distribution.

The results obtained for the two pairs of nitrostilbenes indicated that a second donor reduces fluorescence solvatochromism and that the magnitude of the effect depends in part on the conjugative contact of the second donor with the acceptor group. In the case of DMNI, the second donor, located on a molecular entity relatively insulated from the main chromophore by a large torsional angle (i.e., the 3-aryl ring), does not dramatically change μ_g and α. Thus, the absorption and emission properties of DMNI do not differ much from those of MMNI. Therefore, a second oxygen may be incorported into the 2,3-diarylindene system at this position to decrease lipophilicity, since this is an important consideration in the design of functionalized ligands as biological probes.[44]

If the second donor is essentially copolanar with the main chromophore, as in BIF, μ_g is greatly affected. This change manifests itself in lesser emission solvatochromism and bathochromicity and greater absorption bathochromicity as compared to PNS. The latter characteristic would be desirable in the analysis of biological systems that are photosensitive to short-wavelength irradiation. Thus, a second donor in a fluorophore may alter the absorpion and emission maxima, solvent sensitivity, dipole moment, and lipophilicity, with its position being of critical importance. Such structural effects on fluorescence are of value in the custom design of fluorophores for specific applications.

All four methoxynitrostilbenes diplayed excellent environmental sensitivity, although BIF less so. The estrogen receptor binding properties of the phenolic analogues of DMNI and MMNI and the fluorescence quantum yields of the phenolic analogue of DMNI are described elsewhere.[6b] These compounds may be of interest as general reporter fluorophores and as fluorescent ligands for the many proteins that bind to triarylethylenes.[6a]

(41) Dewar, M. J. S.; Thiel, W. *J. Am. Chem. Soc.* **1977**, *99*, 4899.

(42) Hoffman, R. *Acc. Chem. Res.* **1971**, *4*, 1.

(43) Fabian, W. M. F. *J. Comput. Chem.* **1988**, *9*, 369.

(44) (a) Katzenellenbogen, J. A.; Heiman, D. F.; Carlson, K. E.; Lloyd, J. E. In *Receptor Binding Radiotracers*; Eckelman, W. C., Ed.; CRC Press: Boca Raton, FL, 1982; pp 93–126. (b) Anstead, G. M.; Peterson, C. S.; Katzenellenbogen, J. A. *J. Steroid Biochem.*, in press.

Experimental Section

General. Melting points (uncorrected) were determined on a Thomas-Hoover apparatus. Analytical thin-layer chromatography (TLC) was performed on Merck silica gel F-254 glass-backed plates. Flash chromatography[45] was done using Woelm 32-63 μm silica gel.

Proton nuclear magnetic resonance (^{1}H NMR) spectra were obtained on a Varian XL-200 (200 MHz) or a General Electric QE-300 (300 MHz) spectrometer; chemical shifts are reported downfield from a tetramethylsilane internal standard (δ-scale). Infrared (IR) spectra were obtained in chloroform on a Nicolet 700 spectrometer: prominent and diagnostic peaks are reported. Ultraviolet (UV) spectra were determined with a Hewlett-Packard 8451A spectrophotometer. Low-resolution mass spectra (MS) were done in the electron impact mode on the Varian CH-5 spectrometer. The reported data are for an electron energy of 70 eV and follow the form of *m/z* (intensity relative to base peak = 100). The corrected fluorescence emission spectra were acquired on a Spex Fluorolog 2 (Model IIIC) instrument. Elemental analyses were performed by the Microanalytical Service Laboratory of the University of Illinois. SYBYL Molecular Model System (Version 3.4, Tripos Associated, St. Louis, MO), operating on a Vax 11-750 computer, was used for molecular binding, graphics, volume and empirical force field (MAXIMIN) calculations, and as an interface for MO (AM1) calculations.

Unless otherwise noted, a standard procedure for product isolation as used: quenching by addition of water or an aqueous solution, exhaustive extraction with an organic solvent, washing the extracts, drying with $MgSO_4$, and solvent evaporation under reduced pressure. The quenching media, extraction solvents, and aqueous washes used are noted after the phrase "product isolation".

*Diphenyl (4-Nitrophenylamino)phenylmethanephosphonate (**8**).* 4-Nitroaniline (13.8 g, 0.1 mol) and benzaldehdye (10.6 g, 0.1 mol) were dissolved in benzene (100 mL) and heated at reflux for 24 h. A Dean-Stark trap was used to periodically remove water and wet benzene; fresh benzene was added. Diphenyl phosphite (26 g, 85–90%, about 0.1 mol) was added and the solution was heated at reflux for another 12 h, with intermittent water/wet benzene removal and benzene replenishment. The solvent was evaporated and the solid was triturated with 1:1 Et_2O–EtOAc, providing a pale yellow powder. A second crop was obtained by concentration of the mother liquors and recrystallization (Et_2O, −30 °C). The total yield was 44.8 g (94%): mp 156–157.5 °C; IR 1600, 1490, 1330, 1315, 950 cm^{-1}; ^{1}H NMR ($CDCl_3$) δ 7.98 (d, 2 H, *J* = 9 Hz, Ar *H* ortho to $-NO_2$); 7.60–7.06 (m, 13 H, Ar*H*), 6.73 (d, 2 H, *J* = 8 Hz, Ar*H*), 6.57 (d, 2 H, *J* = 9 Hz, Ar*H*, ortho to −N*H*−), 6.30 (br s, 1 H, −N*H*−), 5.20 (d, 1 H, *J* = 25 Hz, −C*H*−); MS, 460 (1, M^+), 234 (35), 227 (100), 179 (6), 94 (62). Anal. Calcd for $C_{25}H_{21}N_2O_5P$: C, 65.22; H, 4.60; N, 6.08; P, 6.73. Found: C, 65.07; H, 4.62; N, 6.07; P, 6.75.

*1-Phenyl-2-(4-nitrophenyl)ethanone (**9**).* Sodium hydride (50% dispersion in oil, 0.96 g, 0.020 mol) was washed with hexane (20 mL), suspended in THF (50 mL), and cooled to −78 °C. Phosphonate **8** (8.0 g, 0.018 mol) in THF (100 mL) was added dropwise over 2 h, to give a dark orange solution. 4-Nitrobenzaldehyde (2.8 g, 0.018 mol), dissolved in THF (100 mL), was added, and the resulting purple solution was stirred at 25 °C for 12 h. The solvent was evaporated and the dark residue was dissolved in methanol (80 mL) and concentrated HCl (15 mL). The solution was heated at reflux for 1.5 h. Product isolation (H_2O, CH_2Cl_2, saturated $NaHCO_3$) and two recrystallizations from methanol at −30 °C gave 1.72 g (39%) of dark yellow crystals: mp 137–138 °C; ^{1}H NMR ($CDCl_3$) δ 8.20 (d, 2 H, *J* = 8 Hz, Ar*H* ortho to $-NO_2$), 8.02 (d, 2 H, *J* = 8 Hz, Ar*H* ortho to −CO−), 7.62 (t, 1 H, *J* = 7 Hz, Ar*H* para to −CO−), 7.50 (t, 2 H, *J* = 8 Hz, Ar*H* meta to −CO−), 7.43 (d, 2 H, *J* = 8 Hz, Ar*H* meta to $-NO_2$), 4.42 (s, 2 H, $-CH_2-$); MS, 105 (100), 77 (9). Anal. Calcd for $C_{14}H_{11}NO_3$: C, 69.70; H, 4.60; N, 5.81. Found: C, 69.39; H, 4.54; N, 5.70.

*1-Phenyl-2-(4-nitrophenyl)-3-(3-methoxyphenyl)-1-propanone (**10**).* Diisopropylamine (0.54 mL, 4.1 mmol) was dissolved in THF (5 mL) and the solution was chilled to 0 °C. A solution of *n*-butyllithium in hexane (1.6 M, 2.5 mL, 4.1 mmol) was added. After 0.5, h, nitrodeoxybenzoin (**9**) (1.0 g, 4.1 mol) dissolved in THF (20 mL) was added dropwise over 2 h. After an additional 0.5 h, LiI (28 mg, 0.21 mmol) and 3-methoxybenzyl chloride (978 mg, 6.2 mmol) were added. The solution was heated at 40 °C for 8 h. Product isolation (5% HCl, EtOAc, brine) and flash chromatography (9:1 hexane–EtOAc) gave 1.1 g of a yellow oil (80%). The oil solidified on standing, yielding a pale yellow solid: mp 66–69 °C; ^{1}H NMR ($CDCl_3$) δ 8.11 (d, 2 H, *J* = 9 Hz, Ar*H* ortho to $-NO_2$), 7.88 (d, 2 H, *J* = 8 Hz, Ar*H* ortho to −CO−), 7.51 (t, 1 H, *J* = 7 Hz, Ar*H*, para to −CO), 7.39 (d, 4 H, Ar*H* meta to $-NO_2$ and Ar*H* meta to −CO), 7.12 (t, 1 H, *J* = 8 Hz, Ar*H* meta to $-OCH_3$), 6.70 (dd, 1 H, *J* = 8, 2 Hz, Ar*H* para to $-OCH_3$), 6.62 (d, 1 H, *J* = 2 Hz, Ar*H* ortho to $-CH_2-$, $-OCH_3$), 4.94 (t, 1 H, *J* = 7 Hz, −CO−C*H*−ArNO_2), 3.71 (s, 3 H, $-OCH_3$), 3.54 (dd, 1 H, *J* = 14, 7 Hz, $-CH_2-$), 3.07 (dd, 1 H, *J* = 14, 8 Hz, $-CH_2-$); MS, 361 (5, M^+), 256 (3), 121 (4), 105 (100). Anal. Calcd for $C_{22}H_{19}NO_4$: C, 73.12; H, 5.30; N, 3.88. Found: C, 72.97; H, 5.60; N, 3.58.

*2-(4-Nitrophenyl)-3-phenyl-6-methoxyindene (**3**).* Triaryl ketone **9** (0.97 g) was mixed with polyphosphoric acid (PPA, 10 g) and stirred mechanically at 40 °C for 4 h. Product isolation (ice water, EtOAc, saturated $NaHCO_3$), multiple recrystallizations (twice from EtOAc at −30 °C; once from Et_2O–EtOAc at −30 °C), and flash chromatography (9:1 hexane–EtOAc) of the mother liquors provided 636 mg (69%) of a yellow solid: mp 182–183 °C; IR 1590, 1510, 1341, 1224 cm^{-1}; ^{1}H NMR (acetone-d_6) δ 8.03 (d, 2 H, *J* = 9 Hz, Ar*H* ortho to $-NO_2$), 7.54–7.33 (m, 7 H, Ar*H*), 7.19 (s, 1 H, Ar*H* ortho to $-CH_2-$), 7.08 (d, 1 H, *J* = 8 Hz, Ar*H* meta to $-OCH_3$), 6.87 (dd, 1 H, *J* = 8, 2 Hz, Ar*H* para to $-CH_2-$), 4.00 (s, 2 H, $-CH_2-$), 3.83 (s, 3 H, $-OCH_3$); MS, 343 (100, M^+), 328 (6), 312 (2), 300 (2), 297 (3), 282 (3). Anal. Calcd for $C_{22}H_{17}NO_3$: C, 76.95; H, 4.99; N, 4.08. Found: C, 76.77; H, 5.09; N, 3.93.

*(Z)-2-(4-Nitrobenzylidene)-7-(2H)-5-methoxyisobenzofuran (**6**).* 4-Nitrophenylacetic acid (1.0 g, 5.52 mmol) and 3-methoxybenzyl chloride (1.04 g, 6.62 mmol) were mixed with polyphosphoric acid (PPA, 30 g) and stirred mechanically at 60 °C for 3.5 h. Product isolation as for **3** and recrystallization from methanol–acetone at −30 °C yielded an orange solid (750 mg, 50%); an analytical sample was obtained by a second recrystallization from ethanol–acetone at −78 °C: mp 186–188 °C; IR 1645, 1585, 1502, 1335, 1040, 855 cm^{-1}; ^{1}H NMR (DMSO-d_6) δ 8.16 (d, 2 H, *J* = 9 Hz, Ar*H* ortho to $-NO_2$), 7.83 (d, 2 H, *J* = 9 Hz, Ar*H* meta to $-NO_2$), 7.75 (d, 1 H, *J* = 9 Hz, Ar*H* meta to $-OCH_3$), 7.11 (s, 1 H, Ar*H* ortho to $-CH_2$), 7.05 (d, 1 H, *J* = 9 Hz, Ar*H* para to $-CH_2-$), 6.19 (s, 1 H, −C*H*=), 5.61 (s, 2 H, $-CH_2-$), 3.84 (s, 3 H, $-OCH_3$). MS, 283 (100, M^+), 237 (12), 208 (11), 194 (11), 165 (28). Anal. Calcd for $C_{16}H_{13}NO_4$: C, 67.89, H, 4.63; N, 4.94. Found: C, 67.88; H, 4.80; N, 4.84.

Acknowledgment. We are grateful for the support of this research through a grant from the National Institutes of Health (PHS 5R01 DK 15556). High-field NMR spectra were obtained on instruments supported by a grant from the National Institutes of Health (RR 02299). We thank Mr. Rajgopal Srinivasan for helpful discussions.

Registry No. **3**, 114584-04-2; **5**, 114584-03-1; **6**, 124100-04-5; **7**, 4648-33-3; **8**, 19348-89-1; **9**, 3769-82-2; **10**, 124100-05-6; *p*-$NO_2C_6H_4NH_2$, 100-01-6; PhCHO, 100-52-7; $(PhO)_2P(=O)H$, 4712-55-4; *p*-$CHOC_6H_4NO_2$, 555-16-8; *m*-$MeOC_6H_4CH_2Cl$, 824-98-6; *p*-$NO_2C_6H_4CH_2CO_2H$, 104-03-0.

(45) Still, W. C.; Kahn, M.; Mitra, A. *J. Org. Chem.* **1978**, *43*, 2923.